ISSN 1070-3284, Russian Journal of Coordination Chemistry, 2022, Vol. 48, No. 6, pp. 362–370. © Pleiades Publishing, Ltd., 2022.
Russian Text © The Author(s), 2022, published in Koordinatsionnaya Khimiya, 2022, Vol. 48, No. 6, pp. 360–369.

Unsymmetrical Structure of the Co(III) Complex with Bisheteroarylhydrazone as Hydrazone and Quinolone Tautomers Stabilized by Hydrogen Bond

Yu. P. Tupolova[a], *, D. V. Korchagin[b], **, V. E. Lebedev[a], L. D. Popov[a], G. V. Shilov[b], I. N. Shcherbakov[a], V. A. Chetverikova[a], and S. M. Aldoshin[b]

[a] *Southern Federal University, Rostov-on-Don, Russia*

[b] *Institute of Problems of Chemical Physics, Russian Academy of Sciences, Chernogolovka, Moscow oblast, Russia*

**e-mail: yptupolova@sfedu.ru*

***e-mail: korden@icp.ac.ru*

Received September 11, 2021; revised December 6, 2021; accepted December 23, 2021

Abstract—Bisheteroarylhydrazone (H_2L), the product of 2-hydrazinoquinoline condensation with diacetyl, and mononuclear Co(III) complex $[Co(HL)_2]Br·2DMSO$ (**I**) based on this ligand were synthesized. The structure of the chelate was determined by X-ray diffraction (CIF file CCDC no. 2099899). The Co(III) ion in **I** occurs in the low-spin state and has a slightly distorted octahedral coordination unit. The two monodeprotonated bisquinolylhydrazones in the chelate function as tridentrate ligands in different tautomeric forms stabilized by interligand intramolecular hydrogen bond.

Keywords: bisheteroarylhydrazones, quantum chemical modeling, cobalt(III), X-ray diffraction

DOI: 10.1134/S1070328422060069

INTRODUCTION

Hydrazones containing heterocyclic moieties and complexes of these hydrazones are promising synthesis and investigation objects in modern chemistry. This is due, first of all, to the possible practical applications of these compounds. Heteroarylhydrazones are used to obtain biochemical and pharmacological agents, as they exhibit a broad range of physiological activities such as hypotensive, antituberculosis, antitumor, antiviral, antihypertensive, and other types of activity [1–5]. Heteroarylhydrazones are also used as analytical reagents for transition metal ions dyes, and catalysts of some industrial processes [1, 6, 7].

Heteroarylhydrazones are promising ligand systems for the synthesis of complexes with various structures and properties, which are important for the design of magnetoactive, optical, and catalytic materials and pharmaceutical agents [8–19]. It is known that the content of heterocyclic moiety considerably affects the complexing behavior of the ligand system. The broad range of donor atoms and the ability to change the denticity depending on the reaction conditions account for the ability of heteroarylhydrazones to exist in different tautomeric forms, which affects the structure and, hence, the properties of the complexes [20–22]. Therefore, it appears important to identify the factors that affect the formation of particular tautomers of the ligands in the complexes.

This work is devoted to the synthesis and study of a new polydentate ligand system, the product of condensation of 2-hydrazinoquinoline with diacetyl (H_2L), and the heteroleptic complex $[Co(HL)_2]Br·2DMSO$ (**I**), in which two monodeprotonated HL ligands occur as different tautomers owing to the stabilizing interligand intramolecular hydrogen bond.

EXPERIMENTAL

Commercial chemicals were used as the starting reactants. The solvents were purified and dried by standard procedures. 2-Hydrazinoquinoline was synthesized by a reported procedure [23].

Synthesis of H_2L. A solution of diacetyl (0.17 g, 2 mmol) in isopropanol was added to a hot solution of 2-hydrazinoquinoline (0.64 g, 4 mmol) in isopropanol (8 mL). The reaction mixture was heated at reflux for 4.5 h. The resulting yellow crystalline precipitate was collected on a filter and washed with isopropanol. The bisquinolylhydrazone thus formed was recrystallized from butanol. The yield of H_2L was 53%. T_m = 280°C.

For $C_{22}H_{20}N_6$			
Anal. calcd., %	C, 71.72	H, 5.47	N, 22.81
Found, %	C, 71.64	H, 5.51	N, 22.53

IR (ν, cm^{-1}): 3337 w ν(NH), 1616 s, 1606 s ν(C=N), 1572 w, 1463 w, 1429 m, 1377 w, 1287 w, 1244 w, 1154 s, 1135 w, 1120 w, 1017 w, 985 w, 944 w, 903 w, 828 m, 783 w, 760 w.

^{1}H NMR (DMSO-d_6; δ, ppm (*J*, Hz)): 2.32 (s, 6H, CH_3), 7.29 (t, 2H, H^7_{arom}, $^3J_{HH}$ 6.0), 7.59 (t, 2H, H^8_{arom}, $^3J_{HH}$ 6.0), 7.63 (m, 4H, $H^{4,6}_{arom}$), 7.78 (d, 2H, H^9_{arom}, $^2J_{HH}$ 6.0), 8.18 (d, 2H, H^3_{arom}, $^2J_{HH}$ 6.0), 10.21 (s, 2H, NH).

Synthesis of $[Co(HL)_2]Br·2DMSO$ (I). A solution of $CoBr_2·6H_2O$ (0.13 g, 4.1 mmol) in methanol (2 mL) was added to a hot suspension of bisquinolylhydrazone (H_2L) (0.15 g, 4 mmol) in methanol (8 mL). The solution turned dark brown, and after 30 min, a precipitate formed. The reaction mixture was heated at reflux for 4 h. The light brown amorphous precipitate was collected on a filter and washed with methanol. The crystals were grown from DMSO. The yield was 51%, T_m > 280°C.

For $C_{48}H_{40}N_6O_2S_2Co$

Anal. calcd., %	C, 66.57	H, 5.82	Co, 6.81	N, 9.70
Found, %	C, 66.45	H, 5.89	Co, 6.74	N, 9.76

IR (ν, cm^{-1}): 3197 w, 3052 w ν(NH), 1638 m, 1620, 1606 m ν(C=N), 1577 w, 1518 m, 1482 w, 1423 w, 1388 w, 1325 w, 1306 w, 1248 w, 1229 m, 1176 w, 1141 w, 1116 m, 1135 w, 1012 w, 969 w, 943 w, 856 w, 819 m, 771 m, 747 m, 636 w. ^{1}H NMR (DMSO-d_6; δ, ppm (*J*, Hz)): 2.0 (s, 6H, CH_3), 3.11 (s, 6H, CH_3), 7.0–8.5 (m, 24H, H_{arom}), 10.71 (s, 1H, NH), 12.41 (s, 1H, NH).

Elemental analysis was carried out on a Perkin-Elmer 240C instrument at the Laboratory of Microanalysis of the Southern Federal University. ^{1}H NMR spectra were recorded on a Bruker spectrometer, 300 MHz, at 20°C. IR spectra were measured on a Varian Scimitar 1000 FT-IR instrument in mineral oil in the 400–4000 cm^{-1} range.

The magnetic susceptibility of complex **I** was determined by the relative Faraday method at 300 K and a magnetic field strength of 9000 Oe. The setup was calibrated against the complex $Hg[Co(CNS)_4]$.

Quantum chemical calculations were carried out by the density functional theory (DFT) method using the B3LYP hybrid exchange correlation functional [24] in the 6-311++G** split valence basis set of Gaussian functions extended by polarization and diffuse functions on all atoms. The Gaussian'09 software program was used [25]. The geometry was optimized without symmetry constraints; normal vibrations with imaginary frequency were absent for all structures. Data preparation, presentation graphics, and visualization of calculation results were performed using the Chemcraft program [26].

X-ray diffraction analysis was carried out on a XCalibur diffractometer with an EOS CCD detector (Agilent Technologies UK Ltd., Yarnton, Oxfordshire, England). The reflections were collected and unit cell parameters were determined and refined at a temperature of 100(1) K using monochromatic MoK_α radiation with λ = 0.71073 Å by the CrysAlis PRO program [27]. The structure was solved by direct methods. The positions and thermal parameters of non-hydrogen atoms were refined isotropically and then anisotropically by the least squares method. The positions of hydrogen atoms were determined from difference Fourier maps and refined in the riding model. One DMSO solvate molecule is disordered over two positions with 50% occupancy. All calculations were carried out using the SHELXTL program package [28].

Crystallographic parameters and structure refinement details for compound **I** are given in Table 1 and selected interatomic distances and bond angles are in Table 2.

The additional structural data for **I** were deposited with the Crystal Crystallographic Data Centre (CCDC no. 2099899; deposit@ccdc.cam.ac.uk or http://www.ccdc.cam.ac.uk).

RESULTS AND DISCUSSION

Bisheteroarylhydrazone H_2L and Co(III) complex **I** of this ligand were synthesized according to Scheme 1.

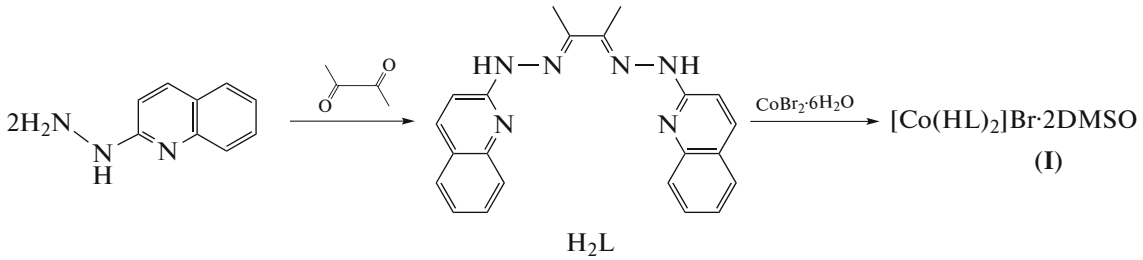

Scheme 1.

Table 1. Crystallographic data, X-ray experiment details, and structure refinement parameters for **I**

Parameter	Value
Molecular formula	$C_{48}H_{50}N_{12}O_2S_2BrCo$
M	1029.96
System	Triclinic
Space group	$P\bar{1}$
Temperature, K	100.0(1)
a, Å	11.4216(4)
b, Å	11.9154(5)
c, Å	18.6368(8)
α, deg	103.947(4)
β, deg	99.148(4)
γ, deg	98.326(3)
V, Å^3	2385.5(2)
Z	2
ρ(calcd.), g/cm^3	1.434
μ, mm^{-1}	1.338
F(000)	1064
Single crystal size, mm	0.4 × 0.2 × 0.15
Range of θ, deg	2.81–29.07
Collected/unique	21725
reflections (R_{int})	12752 (0.0438)
Reflections with $I > 2\sigma(I)$	2199
GOOF	1.013
Number of refined parameters	620
R_1/wR_2 ($I > 2\sigma(I)$)	0.0495/0.0975
R_1/wR_2 (for all reflections)	0.0893/0.1120
$\Delta\rho_{max}/\Delta\rho_{min}$, e Å^{-3}	0.711/–0.591

The composition and the structure of H_2L were determined by elemental analysis and ^{1}H NMR and IR spectroscopy.

The IR spectrum of H_2L shows an absorption band at 3337 cm^{-1} corresponding to NH stretching mode. The ν(C=N) stretching bands corresponding to azomethine groups and quinoline moieties occur at 1616 and 1602 cm^{-1}, respectively.

The ^{1}H NMR spectrum of H_2L contains the following signals: the singlet at 2.3 ppm with 6H intensity for the methyl protons of the diacetyl moiety; a set of 7.3–8.2 ppm signals of 12H intensity for the aromatic protons of the quinoline moieties; and a 2H singlet at 10.21 ppm for the NH groups, which disappears upon the addition of D_2O, indicating the mobility of these hydrogen atoms. This positions of the signals for active $N_{hydr}H$ protons suggests that only symmetrical bishydrazone tautomer (a) exists in solution (see Fig. 1). No bisquinolone tautomer (c) is present in the DMSO solution, since in this case, the $N_{quin}H$ signal would have been shifted downfield owing to the deshielding effect of the heteroaromatic moiety (for example, in the ^{1}H NMR spectrum of 2-quinolone in DMSO-d_6, this signal is observed at 12.6 ppm).

The most stable tautomer of ligand H_2L was identified by quantum chemical modeling of tautomers (a)–(c) using density functional theory (B3LYP6-311++G** level of theory). The total and relative energies of the tautomers in the gas medium were used to evaluate the stability. The form with the lowest total energy was taken as the reference one. The graphical image and the relative energies of the optimized tautomeric forms are shown in Fig. 1.

The results of quantum chemical modeling showed that the symmetrical bishydrazone form (a), in which the hydrogen atoms are located on the nitrogen atoms of the hydrazone moieties, is the most stable. This is in line with experimental results of NMR spectroscopy.

Table 2. Bond lengths (Å) and bond angles (deg) of complex **I**

Bond	*d*, Å	Bond	*d*, Å
Co(1)–N(2)	1.869(2)	Co(1)–N(5)	1.870(2)
Co(1)–N(4)	1.937(2)	Co(1)–N(1)	1.953(2)
Co(1)–N(6)	1.982(2)	Co(1)–N(3)	1.985(2)
N(11)–C(36)	1.359(4)	N(6)–C(27)	1.354(3)
N(11)–N(4)	1.392(3)	N(1)–N(8)	1.391(3)
N(12)–N(5)	1.336(3)	N(9)–N(2)	1.348(3)
N(9)–C(9)	1.358(4)	N(7)–C(18)	1.361(4)
N(7)–C(26)	1.393(3)	N(6)–C(35)	1.388(3)
N(12)–C(27)	1.365(4)	N(10)–C(36)	1.321(3)
N(10)–C(44)	1.382(4)	N(3)–C(9)	1.354(3)
N(5)–C(4)	1.326(3)	N(3)–C(17)	1.383(3)
N(1)–C(1)	1.301(3)	N(4)–C(3)	1.309(3)
N(2)–C(2)	1.307(4)	N(8)–C(18)	1.317(3)
C(25)–C(24)	1.381(4)	C(4)–C(3)	1.438(4)
C(25)–C(26)	1.402(4)	C(4)–C(8)	1.494(4)
C(19)–C(20)	1.344(4)	C(16)–C(15)	1.371(4)
C(19)–C(18)	1.454(3)	C(16)–C(17)	1.405(4)
C(13)–C(14)	1.369(4)	C(14)–C(15)	1.406(4)
C(13)–C(12)	1.403(4)	C(30)–C(31)	1.417(4)
C(29)–C(28)	1.349(4)	C(30)–C(35)	1.423(4)
C(29)–C(30)	1.427(4)	C(1)–C(2)	1.448(3)
C(1)–C(5)	1.487(4)	C(24)–C(23)	1.402(4)
C(3)–C(7)	1.487(4)	C(37)–C(36)	1.438(4)
C(26)–C(21)	1.411(4)	C(20)–C(21)	1.438(4)
C(11)–C(10)	1.349(4)	C(35)–C(34)	1.411(4)
C(11)–C(12)	1.421(4)	C(39)–C(40)	1.409(4)
C(31)–C(32)	1.365(4)	C(39)–C(44)	1.415(4)
C(38)–C(37)	1.349(4)	C(34)–C(33)	1.380(4)
C(38)–C(39)	1.421(4)	C(21)–C(22)	1.404(4)
C(2)–C(6)	1.495(4)	C(23)–C(22)	1.373(4)
C(9)–C(10)	1.430(4)	C(17)–C(12)	1.431(4)
C(27)–C(28)	1.423(4)		
Angle	ω, deg	Angle	ω, deg
N(2)Co(1)N(3)	80.4(1)	N(5)Co(1)N(6)	80.3(1)
N(2)Co(1)N(4)	96.1(1)	N(4)Co(1)N(1)	98.64(9)
N(5)Co(1)N(4)	80.8(1)	N(2)Co(1)N(1)	81.06(9)
N(5)Co(1)N(1)	94.1(1)	N(6)Co(1)N(3)	95.10(9)
N(1)Co(1)N(6)	85.50(9)	N(4)Co(1)N(3)	87.00(9)
N(4)Co(1)N(6)	160.9(1)	N(1)Co(1)N(3)	161.0(1)
N(5)Co(1)N(3)	104.7(1)	N(2)Co(1)N(6)	103.0(1)
N(2)Co(1)N(5)	173.75(9)		

(a)

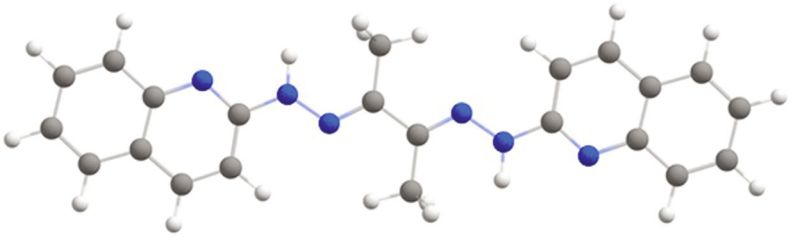

$\Delta E = 0$ kcal/mol

(b)

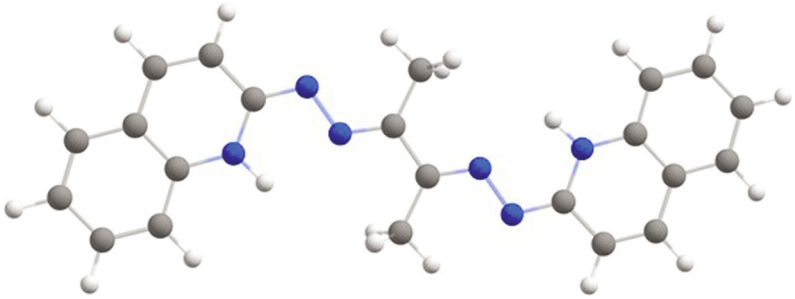

$\Delta E = 5.52$ kcal/mol

(c)

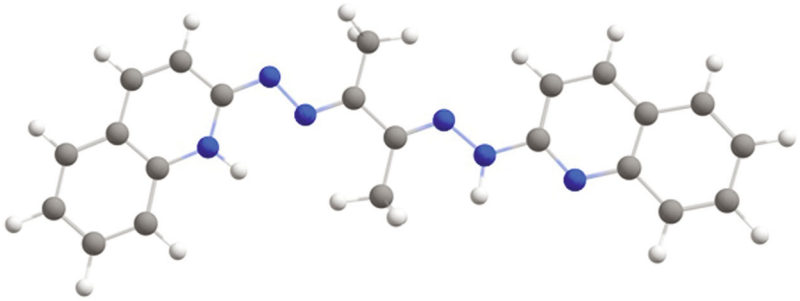

$\Delta E = 3.10$ kcal/mol

Fig. 1. Spatial image and relative energies ΔE in kcal/mol of tautomers (a)–(c) of the ligand H_2L.

The bisquinolone form (b) is the least stable and is destabilized relative to form (a) by 5.52 kcal/mol. The unsymmetrical form (c) in which the proton is located on the hydrazone and quinoline nitrogen atoms is 3.10 kcal/mol less stable. The relatively large energy difference between the tautomers (a)–(c) accounts for the presence of only one isomer (a) in solution.

The reaction of H_2L with cobalt(II) bromide gave $[Co(HL)_2]Br \cdot DMSO$ (**I**), were HL is the monodeptotonated ligand (Scheme 1). This composition and structure of the compound were confirmed by the data of elemental analysis, IR and ^1H NMR spectroscopy, magnetochemistry, and X-ray diffraction.

The IR spectrum of complex **I** exhibits two absorption bands at 3197 and 3052 cm^{-1} corresponding to the NH stretching modes. The C=N stretching bands undergo high-frequency shift by 10–20 cm^{-1}, which attests to coordination of nitrogen atoms of the azomethine and quinoline moieties to the metal ion.

A study of the magnetic susceptibility of complex **I** at room temperature revealed diamagnetic properties characteristic of low-spin Co(III) compounds. This fact indicates that the complex formation is accompanied by Co^{2+} oxidation to Co^{3+}, which often takes place during the formation of octahedral Co(II) complexes with ligands generating a strong crystal field [22]. This is attributable to the fact that low-spin Co^{2+} ion has one unpaired electron in high-lying $d_{x^2-y^2}$ or d_{z^2} orbital ($(t_{2g})^6(e_g)^1$ state); therefore, to attain a more stable $(t_{2g})^6$ state, the Co^{2+} ion easily gives off an electron to the oxidant, being converted to Co^{3+}.

The ^1H NMR spectrum of complex **I** exhibits the following signals: two singlets at 2.0 and 3.11 ppm with 6H intensity each due to the methyl group protons of

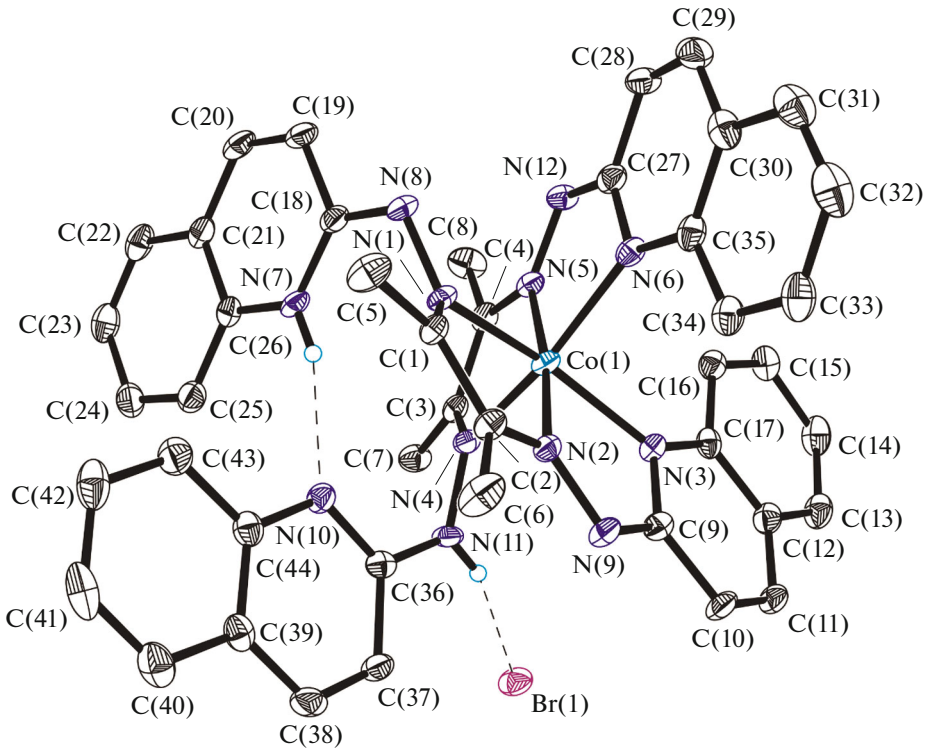

Fig. 2. Molecular structure of compound **I**. The dashed lines show intra- and intermolecular hydrogen bonds. The DMSO solvate molecules and hydrogen atoms not involved in the formation of H-bonds are omitted for clarity.

two diacetyl groups; a set of multiplets at 7.0–8.5 ppm with 24H intensity for the aromatic protons of the quinoline moieties; and two singlets (1H) at 10.71 and 12.41 ppm for the NH protons. The non-equivalence of methyl and NH groups and the shape of aromatic proton signals indicate that the ligands in the complex occur as different tautomers. The relatively small shift of one NH signal in the complex (10.71 ppm) relative to that of H_2L (10.21 ppm) can be attributed to coordination of one of the ligands with retention of the hydrazone tautomeric form, while the pronounced downfield shift of the second signal (12.41 ppm) may be due to the fact that the second ligand exists as the quinolone tautomer.

This assumption is supported by X-ray diffraction data for complex **I**. Figure 2 shows the molecular structure of the compound, which comprises cationic six-coordinate cobalt(III) complex, outer-sphere bromide anion, and two DMSO solvate molecules.

The cationic Co(III) complex is formed by two non-equivalent monodeprotonated bisquinolylhydrazones (HL), which exist as different tautomers both in DMSO solution (as was ascertained independently by ^{1}H NMR spectroscopy) and in the crystalline state. Each ligand performs a tridentate function, despite the presence of numerous coordination options, and nitrogen atoms of one quinoline moiety of each ligand are not coordinated to Co(III), with one of these atoms (N(7)) being protonated and involved in the formation of intramolecular interligand N(7)–H...N(10) hydrogen bond with the other nitrogen atom of the quinoline moiety of the second ligand (Fig. 2). The second ligand exists in the hydrazone form; correspondingly, hydrogen is located at N(11) and, in this case, an intermolecular hydrogen bond with the bromide anion is formed. The geometric characteristics of hydrogen bonds are presented in Table 3.

It can be seen from Table 3 that despite similar donor–acceptor distances for the N(7) atom and the N(4) atom of the hydrazone moiety of the second ligand, the hydrogen bond formed by the N(7)H group is directed towards the heterocyclic N(10) hydrogen atom, as indicated by nearly optimal DHA angle and the H...N(10) distance of 2.152 Å (which is 0.59 Å shorter than the sum of the van der Waals radii of hydrogen and nitrogen). The strength of the N(7)–H...N(10) interligand bond can be assessed by comparing its geometric characteristics with those of other structurally characterized compounds. According to the Cambridge Crystallographic Data Centre (CCDC, version CSD 5.42 with supplements from February to May, 2021), the average D...A and H...A distances for 132 quinolone derivatives that have intermolecular NH hydrogen bonds with heteroaromatic

Table 3. Geometric characteristics of intra- and intermolecular hydrogen bonds in the crystal structure of compound **I**

D–H···A contact	Distance, Å			DHA angle, deg
	D–H	H···A	D···A	
N(7)–H···N(10)	0.81	2.15	2.938(2)	164.5
N(7)–H···N(4)	0.81	2.63	3.165(3)	125.3
N(11)–H···Br(1)	0.83	2.43	3.220(3)	161.5

nitrogen atoms are 3.165 ± 0.205 and 2.357 ± 0.248 Å, respectively. For compound **I**, these distances are much shorter than the average values.

The structural characteristics of the N(7)–H...Br(1) hydrogen bond also attest to its high strength, the DHA angle is close to 180°, and the H...Br(1) distance is 2.427 Å (this is 0.62 Å shorter than the sum of van der Waals radii of hydrogen and bromine atoms). For 20 structures of acyclic hydrazones containing intermolecular NH hydrogen bonds with bromide anions that were found in CCDC, the average N...Br and NH...Br distances are 3.412 ± 0.112 and 2.671 ± 0.164 Å, respectively, which is markedly longer than these distances in compound **I**.

It should be noted that localization of hydrogen at the nitrogen atoms in the ligands correlates with the bond length distribution in their molecules. Indeed, the geometric structures of the ligands coordinated to cobalt(III) in different tautomeric forms are different. Figure 3 shows a comparison of the bond lengths in them. Each of the ligands contains different N–N bonds, one of them, N(1)–N(8) or N(4)–N(11), being single (1.392(3) Å) and the other, N(2)–N(9) or N(5)–N(12), being closer to a double bond (1.347(3) and 1.336(3) Å, respectively). The C(4)–N(5) bond (1.324(3) Å) is longer than similar bonds, which are in the 1.301(3)–1.309(3) Å range. The C(18)–N(8) bond (1.317(3) Å) in the quinolone ligand is markedly shorter than analogous C–N single bonds (1.359(3)–1.365(3) Å). Attention is attracted by elongation of the C–N bonds near the protonated N(7) nitrogen atom (1.361(3) and 1.393(3) Å) compared to the corresponding bonds in the non-protonated uncoordinated quinoline moiety; as expected, they are comparable with those in metal-coordinated quinoline moieties. The coordination of different tautomers of the ligand is additionally supported by the difference between the bond angles at the heteroatom in the protonated and non-protonated quinoline moieties, CN(7)C (123.8(2)°) and CN(10)C (117.4(2)°)

Unlike free molecules, ligands have a nonplanar structure; the quinoline moieties in them occur at angles of 89.2° and 78.3° for ligands in the quinolone and hydrazone forms, respectively. The quinoline moieties of different ligands that are coordinated or not coordinated to the cobalt ion are also approximately perpendicular to each other, 75.2° and 84.9°, respectively.

The Co(III) ion has a distorted octahedral coordination environment formed by nitrogen atoms. The CoN_6 octahedron is somewhat compressed along the N(2)–Co(1)–N(5) direction; the average length of the apical Co–N bond is 1.870(2) Å. In the equatorial plane, the Co–N bond lengths differ insignificantly and are in the 1.937(2)–1.985(2) Å range. The distortion of the ideal octahedral geometry was characterized by octahedral distortion parameters (Σ, Θ, and ζ). The distortion parameters ∑, Θ, and ζ for the cationic complex in compound **I** were 96.73°, 305.36°, and 0.253 Å, respectively; this attests to significant distortions of bond angles (see Table 2) and dihedral angles, with differences between the Co–N bond lengths being moderate (for ideal octahedral complex, Σ = Θ = 0). The structural distortions of the coordination environment of the cobalt(III) ion were also determined using the SHAPE program (2.216 for an octahedron and 9.981 for a trigonal-prismatic environment, where zero means an ideal octahedral geometry). The analysis indicates an unambiguous difference from the trigonal-prismatic environment towards a distorted octahedron.

Considering the charge balance and Co–N bond lengths (Table 2) indicates that the cobalt ion in the complex occurs in the low-spin trivalent state, which is consistent with the diamagnetic properties of this complex.

Figure 4 shows the crystal packing of **I**. Compound **I** crystallizes in the triclinic system, space group $P\bar{1}$. In addition to electrostatic forces, the crystal structure of **I** is stabilized by hydrogen bonds between the bromide anions and the cationic complex molecules and by DMSO solvate molecules; the DMSO oxygen atoms are also involved in intermolecular H-bonds (Fig. 4).

Thus, we synthesized and studied a new polydentate ligand system by condensation of 2-hydrazinoquinoline with diacetyl. According to NMR spectroscopy and quantum chemical modeling, the obtained compound existed in the only bishydrazone tautomer

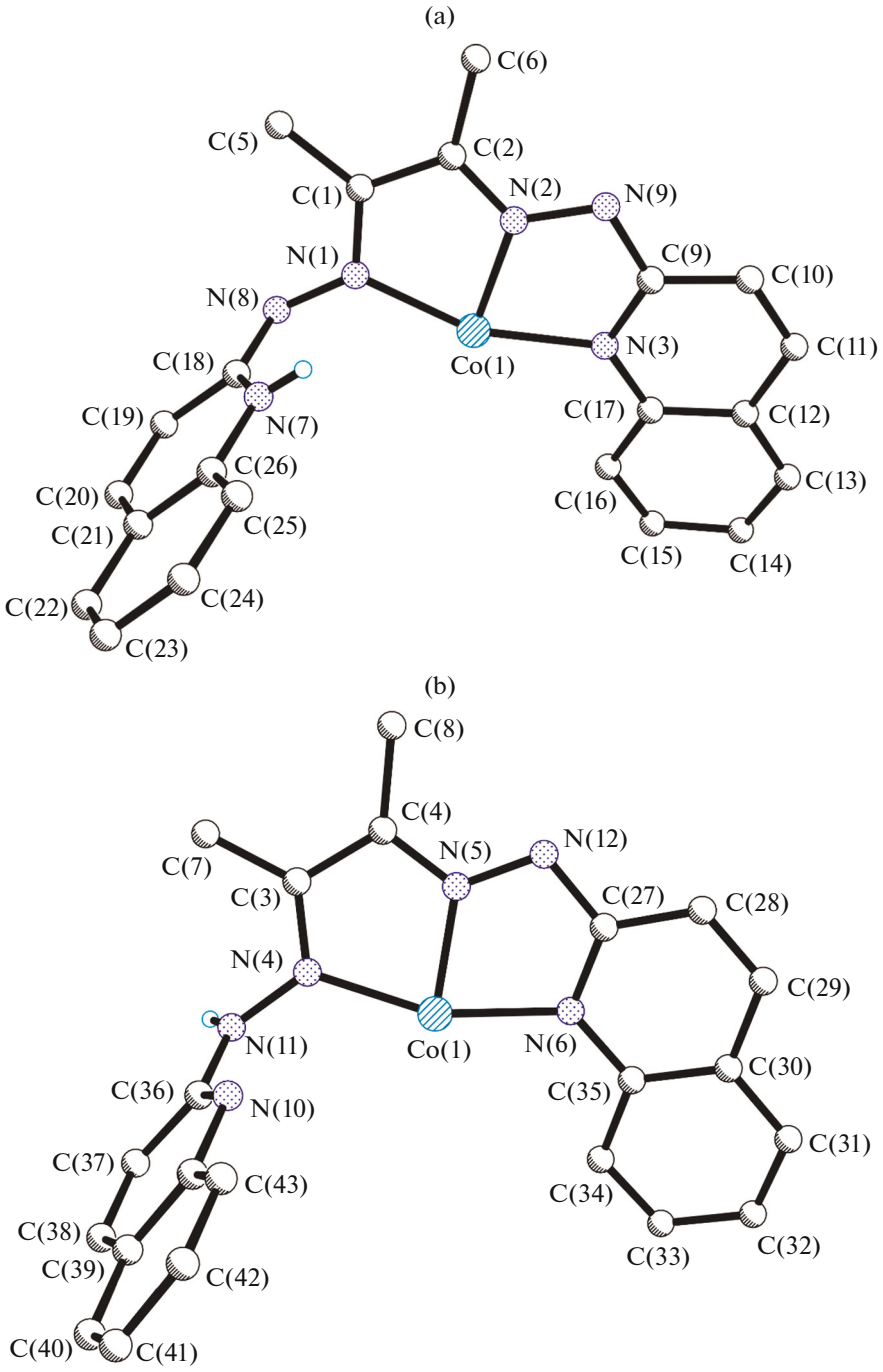

Fig. 3. Ligand coordination in the (a) quinolone and (b) hydrazone forms in the cationic complex in compound **I**.

form. According to X-ray diffraction data, the reaction with cobalt(II) bromide gave an unsymmetrical low-spin Co(III) complex in which two monodeprotonated ligand molecules exist as different tautomers, hydrazone and quinolone ones. The simultaneous existence of different ligand tautomers in the metal chelate is caused by strong hydrogen bonds between the ligands and between one of the ligands and the outer-sphere bromide anion, which stabilize the corresponding tautomers.

ACKNOWLEDGMENTS

X-ray diffraction studies were carried out within the framework of the state assignment of the Ministry of Science and Higher Education of the Russian Federation (no.

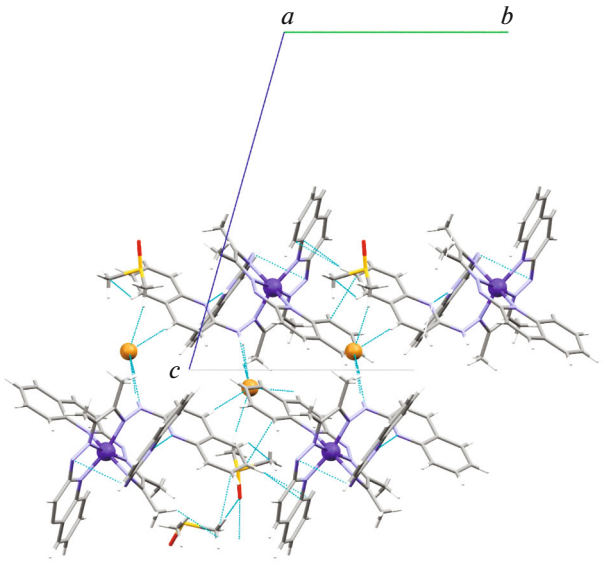

Fig. 4. Crystal packing of **I**: projection on the *bc* crystallographic plane (the dashed lines show intermolecular contacts).

AAAA-A19-119092390076-7) to the Institute of Problems of Chemical Physics, Russian Academy of Sciences.

CONFLICT OF INTEREST

The authors declare that they have no conflicts of interest.

REFERENCES

1. Suvarapu, L.N., Seo, Y.K., Baek, S.O., and Ammireddy, V.R., *J. Chem.*, 2012, vol. 9, p. 1288.
2. Rollas, S. and Küçükgüzel, Ş.G., *Molecules*, 2007, vol. 12, p. 1910.
3. Popp, F.D., *Eur. J. Med. Chem.*, 1989, vol. 24, no. 3, p. 313.
4. Reece, P.A., *Med. Res. Rev.*, 1981, vol. 1, no. 1, p. 73.
5. Bakale, R.P., Ganesh, N.N., Mangannavar, C.V., et al., *Eur. J. Med. Chem.*, 2014, vol. 73, p. 38.
6. Usegi, K., Sik, L.J., Nishioka, H., et al., *Microchem. J.*, 1994, vol. 50, no. 1, p. 88.
7. Singh, R.B., Jain, P., and Singh, R.P., *Talanta*, 1982, vol. 29, no. 2, p. 77.
8. Lukov, V.V., Tsaturyan, A.A., Tupolova, Yu.P., et al., *J. Mol. Struct.*, 2020, vol. 1199, art. 126952.
9. Tupolova, Yu.P., Shcherbakov, I.N., Popov, L.D., et al., *Dalton Trans.*, 2019, vol. 48, no. 20, p. 6960.
10. Lukov, V.V., Tsaturyan, A.A., and Tupolova, Yu.P., et al., *Mendeleev Commun.*, 2019, vol. 29, no. 1, p. 43.
11. Tupolova, Yu.P., Shcherbakov, I.N., Korchagin, D.V., et al., *J. Phys. Chem.*, 2020, vol. 124, no. 47, p. 25957.
12. Popov, L.D., Raspopova, E.A., Borodkin, S.A., et al., *Russ. J. Gen. Chem.*, 2020, vol. 90, no. 3, p. 410. https://doi.org/10.1134/S1070363220030135
13. Levchenkov, S.I., Shcherbakov, I.N., Popov, L.D., et al., *Inorg. Chim. Acta*, 2013, vol. 405, p. 169.
14. Tupolova, Y.P., Levchenkov, S.I., Popov, L.D., et al., *New J. Chem.*, 2021, vol. 45, no. 27, p. 12236.
15. Zelenin, K.N., Khorseeva, L.A., and Alekseev, V.V., *Khim.-Farm. Zh.*, 1992, vol., 26, no. 5, p. 30.
16. Al-Sha'alan, N.H., *Molecules*, 2007, vol. 12, p. 1080.
17. Marzano, C., Pellei, M., Tisato, F., and Santini, C., *Anti-Cancer Agents Med. Chem.*, 2009, vol. 9, p. 185.
18. Santini, C., Maura Pellei, M., Gandin, V., et al., *Chem. Rev.*, 2014, vol. 114, p. 815.
19. Lukov, V.V., Shcherbakov, I.N., Levchenkov, S.I., et al., *Russ. J. Coord. Chem.*, 2019, vol. 45, p. 163. https://doi.org/10.1134/S1070328419030060
20. Tupolova, Y.P., Shcherbakov, I.N., Popov, L.D., et al., *Russ. J. Coord. Chem.*, 2018, vol. 44, p. 132. https://doi.org/10.1134/S1070328418020112
21. Lyubchenko, S.N., Shcherbakov, I.N., Tupolova, Y.P., et al., *Inorg. Chim. Acta*, 2020, vol. 502, art. 119284.
22. Lukov, V.V., Tsaturyan, A.A., Tupolova, Y.P., et al., *New J. Chem.,* 2020, vol. 44, no. 5, p. 2146.
23. Dziomko, V.M., Krasavin, I.A., and Miroshkina, N.I., *Metody polucheniya khimicheskikh reaktivov i preparatov* (Preparation Methods for Chemical Reagents and Agents), 1965, no. 12, p. 50.
24. Becke, A.D., *J. Chem. Phys.*, 1993, vol. 98, no. 7, p. 5648. https://doi.org/10.1063/1.464913
25. Frisch, M.J., *Gaussian 09, Revision A. 02*, 2009.
26. Zhurko, G.A. and Zhurko, D.A., *Chemcraft. Version 1.6* (*build 338*), http://www.chemcraftprog.com.
27. *CrysAlisPro. Version 171.36.20*, Yarnton Oxfordshire: Agilent Technologies, 2011.
28. *SHELXTL. Version 6.14*, Madison: Bruker AXS, 2000.

Translated by Z. Svitanko